AD-A121 819 TRANSIENT PASSIVATION KINETICS OF REACTIVE METAL ELECTRODES I THEORY..(U) AEROSPACE CORP EL SEGUNDO CA CHEMISTRY AND PHYSICS LAB A H ZIMMERMAN 27 SEP 82 1/1

UNCLASSIFIED TR-0082(2945-01)-6 SD-TR-82-78 F/G 9/1 NL

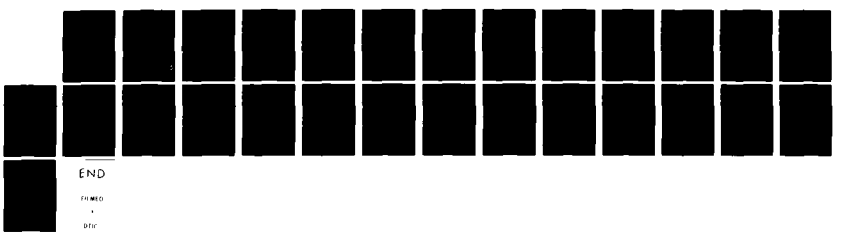

END

FILMED

DTIC

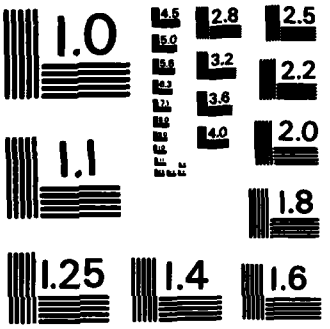

Transient Passivation Kinetics of Reactive Metal Electrodes

I. Theory

A. H. ZIMMERMAN
Chemistry and Physics Laboratory
Laboratory Operations
The Aerospace Corporation
El Segundo, Calif. 90245

27 September 1982

Prepared for

SPACE DIVISION
AIR FORCE SYSTEMS COMMAND
Los Angeles Air Force Station
P.O. Box 92960, Worldway Postal Center
Los Angeles, Calif. 90009

This report was submitted by The Aerospace Corporation, El Segundo, CA 90245, under Contract No. F04701-81-C-0082 with the Space Division, Deputy for Technology, P.O. Box 92960, Worldway Postal Center, Los Angeles, CA 90009. It was reviewed and approved for The Aerospace Corporation by S. Feuerstein, Director, Chemistry and Physics Laboratory. Lt Efren V. Fornoles, SD/YLXT, was the project officer for the Mission-Oriented Investigation and Experimentation (MOIE) Program.

This report has been reviewed by the Public Affairs Office (PAS) and is releasable to the National Technical Information Service (NTIS). At NTIS, it will be available to the general public, including foreign nations.

This technical report has been reviewed and is approved for publication. Publication of this report does not constitute Air Force approval of the report's findings or conclusions. It is published only for the exchange and stimulation of ideas.

Efren V. Fornoles

Efren V. Fornoles, 1st Lt, USAF
Project Officer

Jimmie H. Butler

Jimmie H. Butler, Colonel, USAF
Director of Space Systems Technology

FOR THE COMMANDER

Norman W. Lee

Norman W. Lee, Jr., Colonel, USAF
Deputy for Technology

UNCLASSIFIED

SECURITY CLASSIFICATION OF THIS PAGE (When Data Entered)

REPORT DOCUMENTATION PAGE		READ INSTRUCTIONS BEFORE COMPLETING FORM
1. REPORT NUMBER SD-TR-82-78	2. GOVT ACCESSION NO. AD-A121 819	3. RECIPIENT'S CATALOG NUMBER
4. TITLE (and Subtitle) TRANSIENT PASSIVATION KINETICS OF REACTIVE METAL ELECTRODES. I. THEORY		5. TYPE OF REPORT & PERIOD COVERED 6. PERFORMING ORG. REPORT NUMBER TR-0082(2945-01)-6
7. AUTHOR(s) A. H. Zimmerman		8. CONTRACT OR GRANT NUMBER(s) F04701-81-C-0082
9. PERFORMING ORGANIZATION NAME AND ADDRESS Laboratory Operations The Aerospace Corporation El Segundo, California 90245		10. PROGRAM ELEMENT, PROJECT, TASK AREA & WORK UNIT NUMBERS
11. CONTROLLING OFFICE NAME AND ADDRESS Space Division Air Force Systems Command Los Angeles, California 90009		12. REPORT DATE 27 September 1982 13. NUMBER OF PAGES 22
14. MONITORING AGENCY NAME & ADDRESS(if different from Controlling Office)		15. SECURITY CLASS. (of this report) Unclassified 15a. DECLASSIFICATION/DOWNGRADING SCHEDULE

16. DISTRIBUTION STATEMENT (of this Report)

Approved for public release; distribution unlimited.

17. DISTRIBUTION STATEMENT (of the abstract entered in Block 20, if different from Report)

18. SUPPLEMENTARY NOTES

19. KEY WORDS (Continue on reverse side if necessary and identify by block number)

Battery
Cell
Electrode films
Impedance
Metals
Passivity
Transients

20. ABSTRACT (Continue on reverse side if necessary and identify by block number)

A chemical model is presented that describes the voltage delay often observed when an anodizing current is applied to a highly reactive metal electrode. The model considers the metal surface to be initially covered by a protective film that is disrupted by the passage of anodic current. Relaxation of the surface coverage causes a rise in electrode potential during the initial stages of anodization. The faradaic impedance represented by this model is calculated, and the dependence of the impedance on the rate constants and

DD FORM (FACSIMILE) 1473

UNCLASSIFIED

SECURITY CLASSIFICATION OF THIS PAGE (When Data Entered)

15. KEY WORDS *(Continued)*

20. ABSTRACT *(Continued)*

coverage parameters is examined. For this model, it is shown that voltage delay should exist only when the rate of surface-coverage relaxation is less than the rate of the principal charge transfer process.

CONTENTS

FIGURES

TABLE

I. INTRODUCTION

The use of highly reactive metals such as lithium, aluminum, or zinc for battery electrodes is quite attractive because of their intrinsically high energy densities. However, along with the high reactivity of the metals comes the problem of protecting the metal surface from reaction with the solvent while maintaining high electrochemical activity. Typically, a protective film forms on the metal surface and limits further reaction between metal and solvent. The protective film usually results from a corrosion reaction and should not necessarily be considered the same as passivating films that may form on metal surfaces as products of anodization. The electrode may not work effectively if the film provides much additional electrochemical impedance to the charge transfer process. The impedance of a surface film presents a particularly significant problem when high current loads are applied to the electrode, since the film must be disrupted before effective operation can take place. This problem typically is indicated by a sudden fall in voltage when the load is applied, followed by a rise in voltage to usable levels as the protective film is disrupted -- a phenomenon often termed "voltage delay" in the battery literature.* A preconditioning procedure may sometimes be used to minimize voltage delay. It involves discharging the electrode for some period of time prior to applying the high current load, and may disrupt the film. If the load is applied before substantial film reformation occurs, the voltage delay will be reduced.

This study has two purposes. The first is to gain an understanding of the chemical and physical processes at electrode surfaces that control the voltage-delay phenomenon. We examine those processes on several metals commonly used as battery electrodes, and analyze the kinetics of the voltage delay in relation to reaction rates, as well as to film structures and

*Y. Gerenov, F. Schwager, and R. H. Muller, Electrochemical Studies of the Film Formation on Lithium in Propylene Carbonate Solution Under Open Circuit Conditions, LBL-12102, Lawrence Berkeley Laboratory, Berkeley, Calif. (April 1981).

composition. This report presents the initial theoretical groundwork for analyzing voltage-delay data. The process considered involves an initially film-covered surface that is disrupted either physically or electrochemically by the passage of current. The kinetics of the film formation/disruption processes are investigated in some detail, and equations are developed for evaluating experimental data.

The second purpose of this study is to develop an understanding of the parameters that control the severity of voltage delay. A fundamental understanding of the mechanisms that give rise to voltage delay, coupled with the parametric data, should establish the conditions that minimize voltage delay in battery systems.

II. THEORY

The following three reactions describe a general film formation/disruption process occurring in conjunction with an electrochemical reaction:

$$M(c) + A + mB^- \overset{K_1}{\rightarrow} AB_m + M + me^- \quad (1)$$

$$M + pC^- \overset{K_2}{\rightarrow} MC_p + pe^- \quad (2)$$

$$2M + D \overset{K_3}{\rightarrow} MD + M(c) \quad (3)$$

In reactions (1) through (3), M denotes the metal surface; M(c), the film-covered metal surface; and A, B^-, C^-, and D, generalized chemical reagents. The number of electrons transferred in reactions (1) and (2) are m and p, respectively. Reaction (1) signifies either electrochemical or physical disruption of surface coverage as a result of charge transfer. For physical disruption of the coverage, A is the metal; and for electrochemical disruption, A is the reagent covering the surface. Reaction (2) is the electrode reaction that oxidizes the exposed metal surface and discharges the battery half-cell. Reaction (3) is a chemical corrosion process that regenerates the metal surface coverage. If the relative surface coverage is θ, and β is the maximum superficial density of the surface film in mol/cm^2, the anodic current may be written as

$$\frac{I}{F} = - mK_1\beta\theta[B^-]^m - pK_2\beta(1 - \theta)[C^-]^p \quad (4)$$

where F is Faraday's constant. In Eq. (4) it is assumed that reactions (1) through (3) are elementary reaction steps in the sense that they describe the kinetic dependence of the system on composition, concentrations, and surface coverage. The rate of surface-coverage change is given by

$$\beta \frac{d\theta}{dt} = - K_1 \beta \theta [B^-]^m + K_3 \beta (1 - \theta)[D] \qquad (5)$$

which may be rewritten as

$$\frac{d\theta}{dt} = K_3[D] - \theta\{K_1[B^-]^m + K_3[D]\} \qquad (6)$$

The rate constants K_1 and K_2 are assumed to be voltage dependent as defined by Tafel's law:

$$K_i = k_i \exp(-b_i V) \qquad (7)$$

where k_i and b_i are constants and V is potential. The surface coverage θ is a function of time and voltage, as obtained by integration of Eq. (6),

$$\theta(V,t) = (\theta_i - \theta_f)\, e^{-Gt} + \theta_f \qquad (8)$$

where $G = K_1[B^-]^m/(1 - \theta_f)$, θ_i is the initial surface coverage, $\theta_f = \gamma/(1 + \gamma)$ is the final surface coverage, and $\gamma = K_3[D]/K_1[B^-]^m$.

A. FARADAIC IMPEDANCE TO A VOLTAGE STEP

The faradaic impedance for reactions (1) through (3) may be determined from the response of the system to a change in potential, $\Delta V = V_i - V_f$:

$$\frac{\Delta I}{F} = - m\beta[B^-]^m \Delta(K_1\theta) - p\beta[C^-]^p \Delta[(1 - \theta)K_2] \qquad (9)$$

Equation (7) allows the response ΔI to be expressed as a function of the surface coverage $\theta(V,t)$ and the partial currents I_1 and I_2:

$$\Delta I = I_2(V_f) - I_2(V_i) + \theta(V_i,t)\, I_{12}(V_i) - \theta(V_f,t)\, I_{12}(V_f) \qquad (10)$$

where

$$I_1(V) = mF\beta[B^-]^m k_1 \exp(-b_1V) \qquad (11a)$$

$$I_2(V) = pF\beta[C^-]^p k_2 \exp(-b_2V) \qquad (11b)$$

$$I_{12}(V) = I_2(V) - I_1(V) \qquad (11c)$$

The time dependence may be expressed explicitly by combining Eqs. (8) and (10),

$$\Delta I = U_1 + U_2 \exp[-G(V_i)t] + U_3 \exp[-G(V_f)t] \qquad (12)$$

where

$$U_1 = I_2(V_f) - I_2(V_i) + \theta_f(V_i)\, I_{12}(V_i) - \theta_f(V_f)\, I_{12}(V_f) \qquad (13a)$$

$$U_2 = I_{12}(V_i)\, [\theta_i - \theta_f(V_i)] \qquad (13b)$$

$$U_3 = - I_{12}(V_f)\, [\theta_i - \theta_f(V_f)] \qquad (13c)$$

The faradaic impedance Z_F as a function of frequency is defined as

$$\frac{1}{Z_F(\omega)} = \frac{\Delta I(\omega)}{\Delta V(\omega)} \qquad (14)$$

The Laplace transforms of the voltage step perturbation and the current response in Eq. (12) may be substituted in Eq. (14) to give

$$\frac{1}{Z_F(\omega)} = \frac{U_1}{\Delta V} + \frac{j\omega U_2}{\Delta V[j\omega + G(V_i)]} + \frac{j\omega U_3}{\Delta V[j\omega + G(V_f)]} \qquad (15)$$

The equivalent circuit for an impedance of this form is displayed in Fig. 1. The impedance of the equivalent circuit of Fig. 1 is most conveniently written as

$$\frac{1}{Z_F(\omega)} = \frac{1}{R_1} + \frac{j\omega C_2}{1 + j\omega\tau_2} + \frac{j\omega C_3}{1 + j\omega\tau_3} \qquad (16)$$

The capacitances C_2 and C_3 may take on negative values if U_2 or U_3 in Eqs. (13b) and (13c) are negative, and therefore the net impedance of this equivalent circuit may be inductive under some conditions.

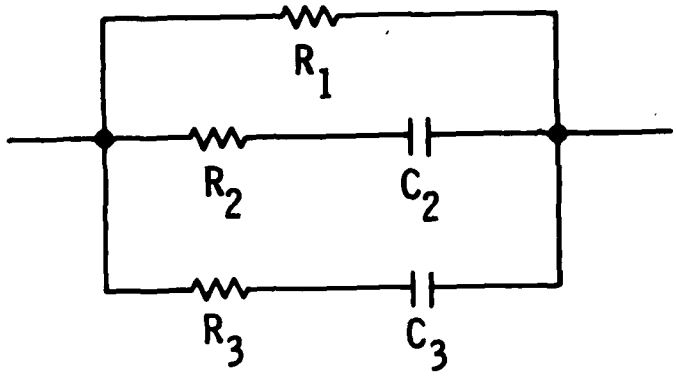

$$R_1 = \frac{\Delta V}{U_1} \qquad R_2 = \frac{\Delta V}{U_2} \qquad R_3 = \frac{\Delta V}{U_3}$$

$$\tau_2 = R_2C_2 = \frac{1}{G(V_i)} \qquad R_3C_3 = \frac{1}{G(V_f)} = \tau_3$$

Figure 1. Equivalent Circuit for Faradaic Impedance

Often impedance is measured under conditions in which only small changes in the voltage occur during the measurement. Under such conditions the above analysis of the impedance to a voltage step may be simplified somewhat:

$$\Delta I = \beta F \Delta V \{p[C^-]^p \, k_2 b_2 [1 - \theta(t)] + m[B^-]^m \, k_1 b_1 \, \theta(t)\} \qquad (17)$$

Here it is assumed that ΔV is sufficiently small such that θ may be approximated as a function of time only, and that the voltage in Eq. (7) is permitted to change only a small amount from its equilibrium value (linear approximation). In this case the impedance is given by the equivalent circuit of Fig. 1, where R_3 and C_3 are no longer present, and

$$R_1 = \left(\beta F\{p[C^-]^p\ k_2 b_2(1 - \theta_f) + m[B^-]^m\ k_1 b_1 \theta_f\}\right)^{-1} \qquad (18a)$$

$$R_2 = \left(\beta F(\theta_i - \theta_f)\ \{k_1 b_1 m[B^-]^m - k_2 b_2 [C^-]^p\}\right)^{-1} \qquad (18b)$$

$$\tau_2 = R_2 C_2 = \frac{1}{G} \qquad (18c)$$

This result is particularly useful because these equivalent-circuit elements are independent of ΔV. Therefore this equivalent circuit is valid for impedance measurements that apply a current-step perturbation to the electrode while monitoring the electrode voltage response, as long as the voltage changes only a small amount from the equilibrium voltage.

B. FARADAIC IMPEDANCE TO A CURRENT STEP

The faradaic impedance of reactions (1) through (3) when a current step ΔI is applied to the electrode may be determined from Eq. (4):

$$\Delta I = - mF\beta[B^-]^m\ K_1(V,t)\ \theta(V,t) - pF\beta[C^-]^p\ K_2(V,t)\ [1 - \theta(V,t)] \qquad (19)$$

Since in this case the voltage is not controlled, it is in general a function of time, and therefore K_1, K_2, and θ are functions of both voltage and time. Equation (19) must be solved numerically by a successive approximation technique to yield the general response $\Delta V(t)$ to a current step ΔI. A numerical Laplace transform of $\Delta V(t)$ allows the faradaic impedance to the current step to be calculated using Eq. (14), and it permits calculation of the voltage function observed when a load is suddenly switched on.

The procedure of numerical analysis is rather cumbersome and may be simplified in situations for which only small changes from the equilibrium voltage occur as a result of the current step. The equivalent circuit in this

case is the same as in the case of a small voltage step, as defined by Eq. (18). In that region of ΔV and ΔI, the equivalent-circuit elements are independent of both ΔI and ΔV and are functions of surface coverages and kinetic parameters only. The linear approximation that may be made in the case of small changes in voltage allows the time dependence of ΔV to be expressed as

$$\Delta V(t) = \frac{\Delta I}{\beta F\{m[B^-]^m k_1 b_1 \theta + p[C^-]^p k_2 b_2 (1 - \theta)\}} \qquad (20)$$

where the time dependence is governed by the variation of θ with time.

C. OVERALL ELECTRODE IMPEDANCE

The overall impedance of a metal electrode, indicated in the equivalent circuit below, includes contributions from the double-layer capacitance C_{DL}, electrolyte resistance R_s, and the impedance arising from diffusion of reagents at the surface Z_D, as well as the faradaic impedance Z_F.

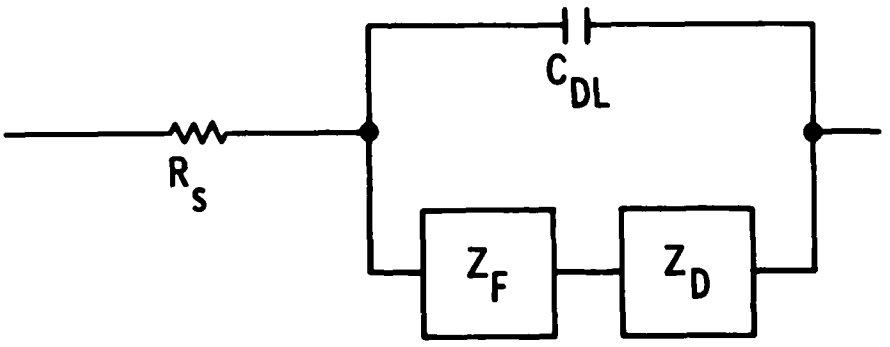

The faradaic impedance is given by Eq. (15), and the diffusion impedance is most conveniently expressed as

$$Z_D = \sigma \omega^{-1/2} (1 - j) \tanh \left[\delta \left(\frac{j\omega}{D}\right)^{1/2}\right] \qquad (21)$$

where σ is a Warburg coefficient; δ, the thickness of the diffusion layer; and D, the diffusion coefficient for the diffusing species. In the calculations in the next section, the contribution from Z_D will be neglected for simplicity.

III. RESULTS

Several approximations may be used to simplify the treatment presented in Sections I and II. The foremost of these can be made when only small voltage changes occur during the measurement of electrode impedance. To determine the range of usefulness of this linear approximation, Table 1 compares the equivalent circuit of the linear approximation with the actual equivalent circuit for different voltage changes. For the approximation to be within 10 percent of the actual circuit, ΔV must be 15 to 20 mV or less. A second approximation that is helpful is to assume that θ is a function of time only. This assumption allows Eq. (12) to be simplified so that

$$\Delta I = U_1' + U_2' e^{-Gt} \tag{22}$$

$$U_1' = I_2(V_f) - I_2(V_i) + \theta_f [I_{12}(V_i) - I_{12}(V_f)] \tag{23a}$$

$$U_2' = (\theta_i - \theta_f) [I_{12}(V_i) - I_{12}(V_f)] \tag{23b}$$

These simplifications allow R_3 and C_3 to be eliminated from the equivalent circuit of Fig. 1. Figure 2 indicates the maximum change in coverage θ [from Eq. (8)] as a function of change in voltage ΔV. The maximum change occurs, approximately, at

$$t = \ell n \frac{G(V_i)/G(V_f)}{G(V_i) - G(V_f)} \tag{24}$$

as long as θ_f is relatively small. The results of Fig. 2 indicate that, for large changes in surface coverage, errors of only several percent or less will

Table 1. Comparison of Linear Approximation [Eq. (18)] to Exact Model (Fig. 1) for Various Voltage Changes ΔV: $b_1 = b_2 = (0.12\ V)^{-1}$, $k_2 = 1.2 \times 10^5\ cm^6 \times mol^{-2}\ sec^{-1}$, $k_1/k_2 = 0.5$, $\beta = 4.4 \times 10^{-8}\ mol/cm^2$, $m = p = 2$, $[B^-] = [C^-] = 7 \times 10^{-3}\ mol/cm^2$, $\theta_i = 1.0$, $\theta_f = 0.02$.

ΔV (volts)		0.005	0.025	0.125
Linear approximation				
R_1	(Ω)	2.427	2.427	2.427
$(1/R_2 + 1/R_3)^{-1}$	(Ω)	-4.839	-4.839	-4.839
τ	(sec)	0.338	0.338	0.338
Exact solution				
R_1	(Ω)	2.358	2.163	1.365
R_2	(Ω)	0.202	1.034	5.042
τ_2	(sec)	0.338	0.338	0.338
R_3	(Ω)	-0.193	-0.818	-1.771
τ_3	(sec)	0.324	0.275	0.120
$(1/R_2 + 1/R_3)^{-1}$	(Ω)	-4.717	-4.340	-2.730
% error		2.9	12.2	77.8

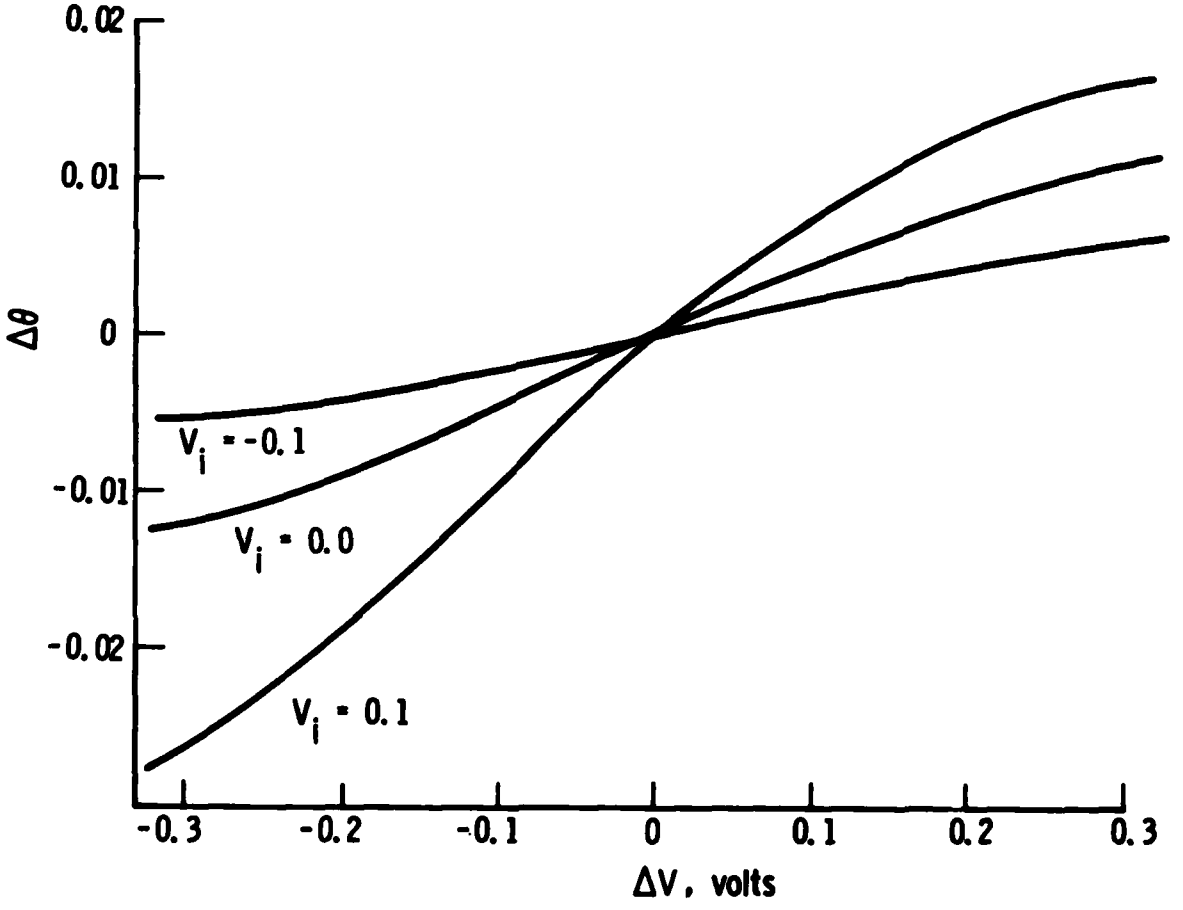

Fig. 2. Relative Surface Coverage Change as Function of Potential Change for Different Initial Potentials: $t = \ln(G_i/G_f)/(G_i - G_f)$, $k_1 = 6 \times 10^4$ $(cm^3/mol)^m$ sec^{-1}, $b_1 = (0.12\ V)^{-1}$, $[B^-]^m = 49 \times 10^{-6}$ $(mol/cm^3)^m$, $\theta_i = 1.0$, $\theta_f = 0.02$.

result when θ is assumed to be independent of voltage. This assumption is not generally valid if $\Delta\theta$ is small, θ_f is large, or ΔV is more than several hundred millivolts.

The dependence of the faradaic impedance on ΔV was determined and tabulated in Table 1. The total electrode impedances for the values of ΔV in Table 1 are indicated in Fig. 3, in which the negative of the reactive component of the impedance is plotted as a function of the resistive component of the impedance, with frequency a running variable. In that plot the upper quadrant corresponds to capacitance and the lower quandrant, inductance. A double-layer capacitance of 200 $\mu F/cm^2$ and an electrolyte resistance of 0.2 Ω were assumed. The linear approximation to the impedance [Eqs. (18a) through (18c)] is closely approximated by curve A in the figure. The primary effect of increasing ΔV is to decrease the high-frequency limit of the faradaic impedance R_{HF},

$$R_{HF} = \frac{\Delta V}{U_1 + U_2 + U_3} \tag{25}$$

below the value expected from the linear approximation $R_{HF\ell}$,

$$R_{HF\ell} = \left[\beta F \left(p[C^-]^p \, k_2 b_2 + \theta_i \left\{ m[B^-]^m \, k_1 b_1 - p[C^-]^p \, k^2 b^2 \right\} \right) \right]^{-1} \tag{26}$$

The value of R_{HF} in Fig. 3 is essentially the diameter of the semicircle in the upper (capacitive) quadrant. The phenomenon of voltage delay is experimentally indicated by an inductive component to the impedance; i.e., the impedance decreases as time progresses or frequency decreases. The inductive impedance may result from a negative capacitance and resistance in the equivalent circuit.

The conditions under which the impedance calculated from this model may be inductive and give rise to voltage delay are of interest. From Eq. (18b)

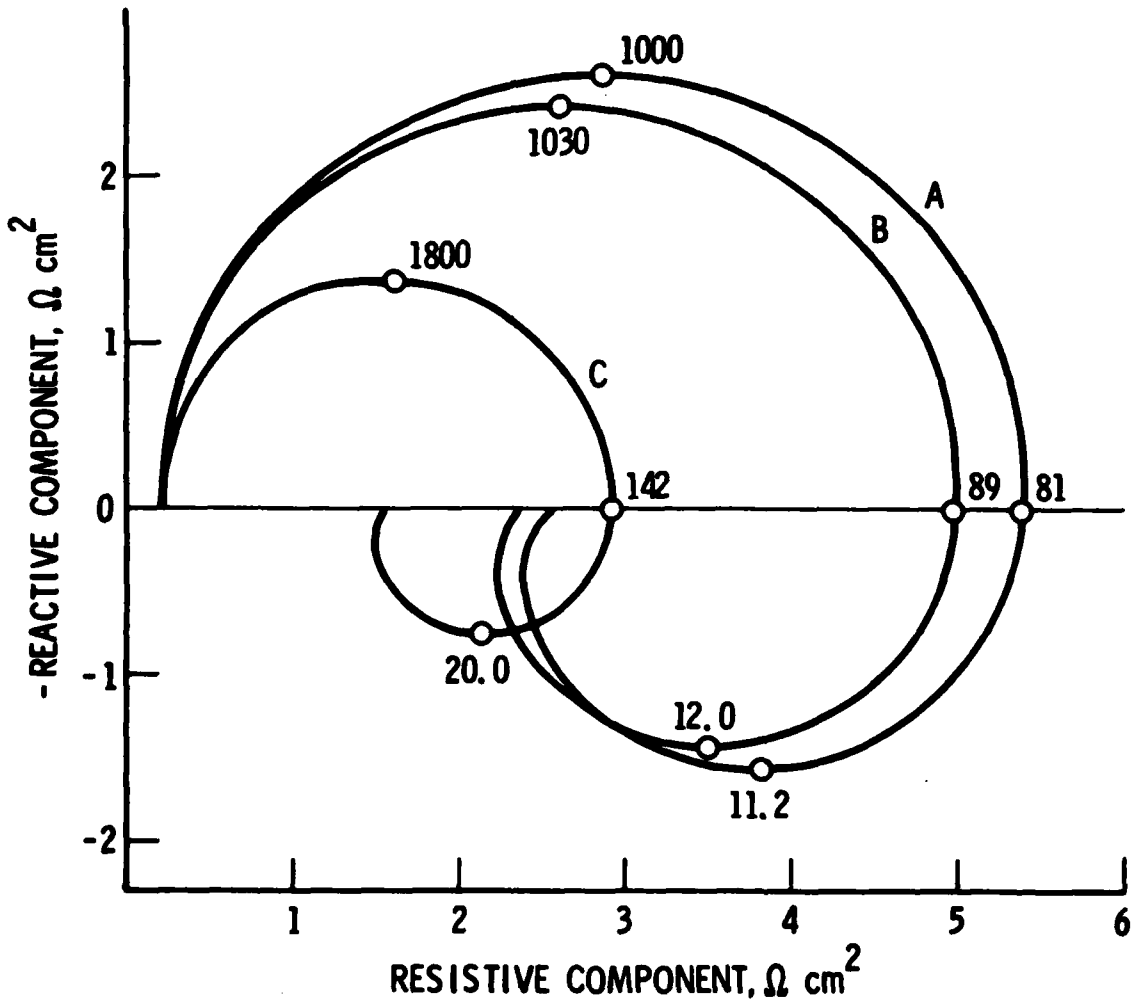

Fig. 3. Electrode Impedance for Data in Table 1. For curve A, ΔV = 5 mV, curve B, ΔV = 25 mV, curve C, ΔV = 125 mV; R_s = 0.2 Ω, C_{DL} = 200 μF/cm². Numbers indicate angular frequencies of reactive extrema and nodes in impedance.

the most obvious and dramatic way to obtain a negative resistance (linear approximation) is for $k_1 b_1 m[B^-]^m < k_2 b_2 p[C^-]^p$. This situation is physically equivalent to requiring that the net current be initially controlled by the rate of reaction (1), which is the process that reduces surface coverage. Figure 4 indicates the electrode impedance for various ratios of k_1 to k_2. A net inductance, or voltage delay, is observed only when $k_1 < k_2$, assuming $b_1 m[B^-]^m = b_2 p[C^-]^p$. When $k_1 = k_2$, the faradaic impedance has no net reactance, thus the electrode impedance reduces to a simple RC equivalent circuit. As k_1 becomes greater than k_2, the charge transfer resistance of reaction (2) begins to control the impedance, and it becomes capacitive at all frequencies.

It is also instructive to examine the effects of different values of θ_i and θ_f, the initial and final surface coverages, on the electrode impedance. For an active metal electrode that is initially in the open-circuit state and subjected to a load at an initial time, it is most likely that the initial surface coverage is nearly complete and that the final surface coverage is somewhat less than complete. The impedance (linear approximation) for an electrode of this kind is illustrated in Fig. 5 for an initial coverage of 1 and final coverages of 0, 0.5, and 0.9. As $\Delta\theta$ decreases, the low-frequency impedance R_l decreases without affecting R_{HF}. For the parameters used in calculating the three curves in Fig. 5, R_l is proportional to $[k_2 + \theta_f(k_1 - k_2)]^{-1}$ and $R_{HF\ell}$ is proportional to $[k_2 + \theta_i(k_1 - k_2)]^{-1}$. Also included in Fig. 5 is the impedance calculated when $\theta_i < \theta_f$.

The voltage response obtained when a load is applied to an electrode must be calculated numerically as indicated in Section II.B, except in the case of small voltage changes, when Eq. (20) may be used. For larger voltage changes the electrode response to a step change in current is best calculated from a numerical solution of Eq. (19), with the double-layer charging term C dV/dt added to the right-hand side. The voltages as a function of time for current changes of 5, 20, and 80 mA/cm^2 are plotted in Fig. 6. The voltage delay is present even for small current changes. Although it increases rapidly as the current change increases, the voltage-delay magnitude increases more slowly than does the voltage drop across a purely resistive element.

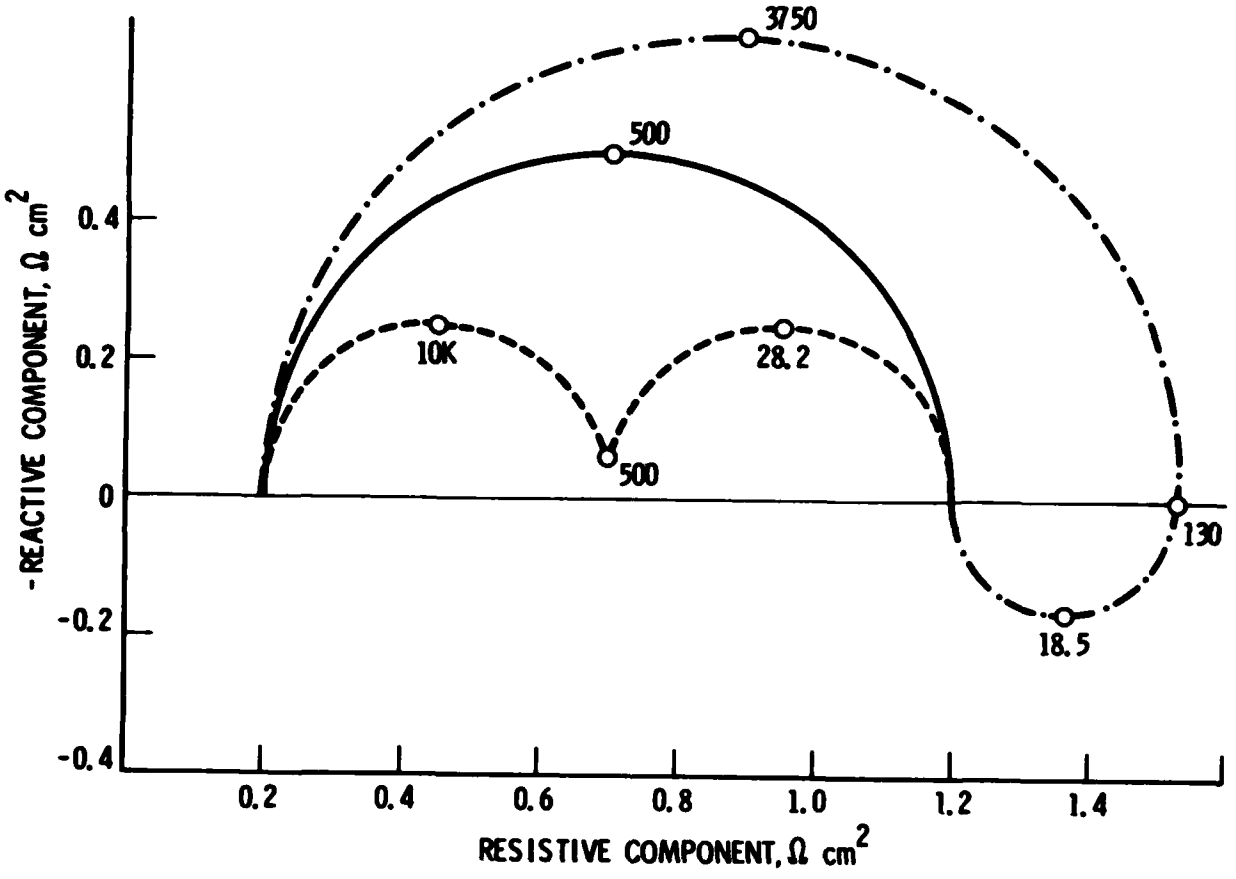

Fig. 4. Electrode Impedance for Different k_1/k_2 Ratios: $k_1/k_2 = 2$ is dashed line, $k_1/k_2 = 1$ is solid line, $k_1/k_2 = 0.5$ is dashed-dotted line. $b_1 = b_2 = (0.12\ V)^{-1}$, $k_2 = 5.77 \times 10^5\ (cm^3/mol)^p\ sec^{-1}$, $\beta = 4.4 \times 10^{-8}\ mol/cm^{-2}$, $p[C^-]^p = m[B^-]^m = 49 \times 10^{-6}\ (mol/cm^3)^p$, $\theta_i = 1.0$, $\theta_f = 0.0$, $R_s = 0.2\ \Omega$, $C_{DL} = 200\ \mu F/cm^2$. Numbers indicate angular frequencies of reactive extrema and nodes.

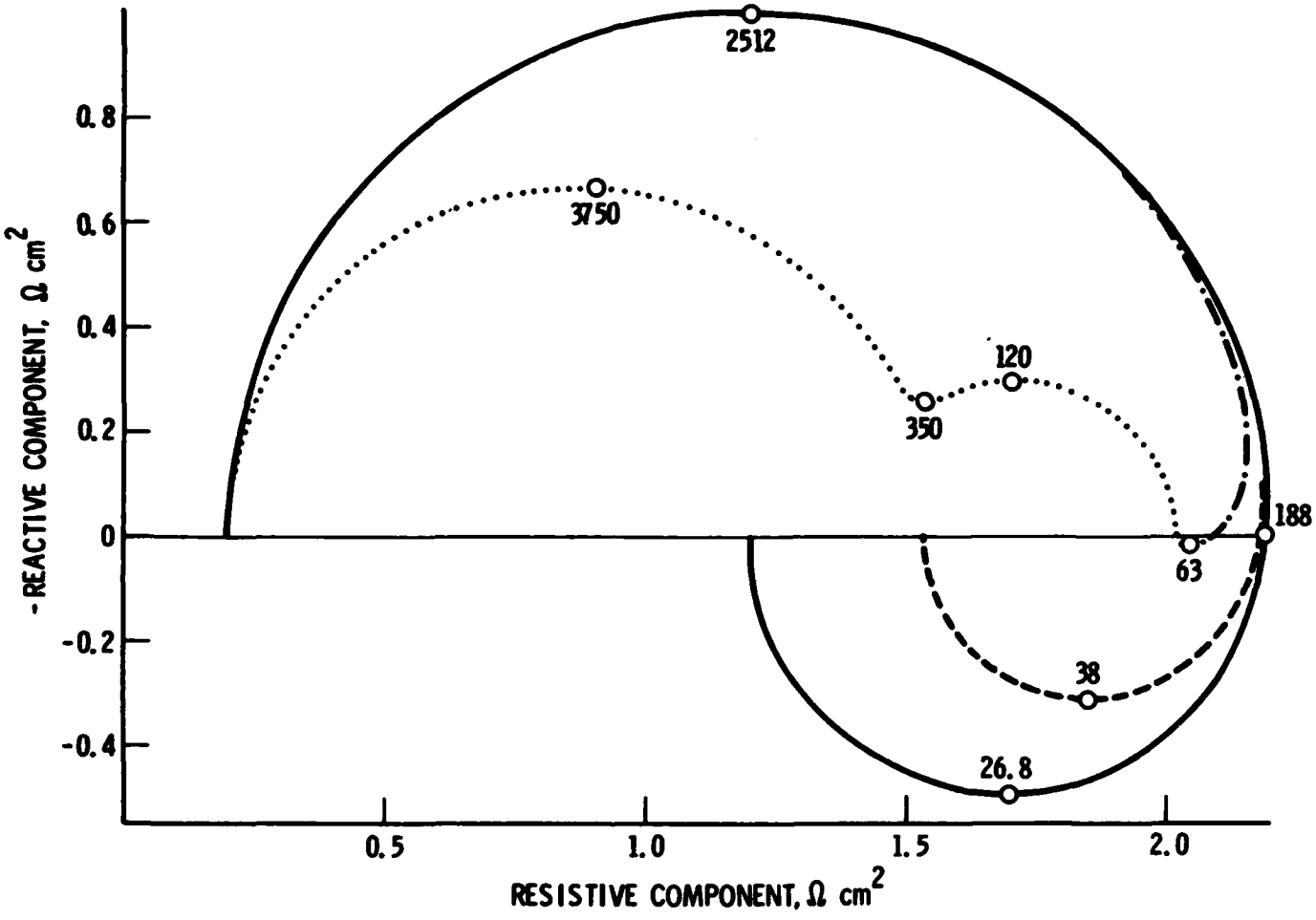

Fig. 5. **Electrode Impedance for Different Surface Coverages. For solid line, $\theta_i = 1$ and $\theta_f = 0$; dashed line, $\theta_i = 1$ and $\theta_f = 0.5$; dashed-dotted line, $\theta_i = 1$ and $\theta_f = 0.9$; dotted line, $\theta_i = 0.5$ and $\theta_f = 0.9$. Other parameters are same as in Fig. 4, with $k_1/k_2 = 0.5$. Numbers indicate angular frequencies of reactive extrema and nodes.**

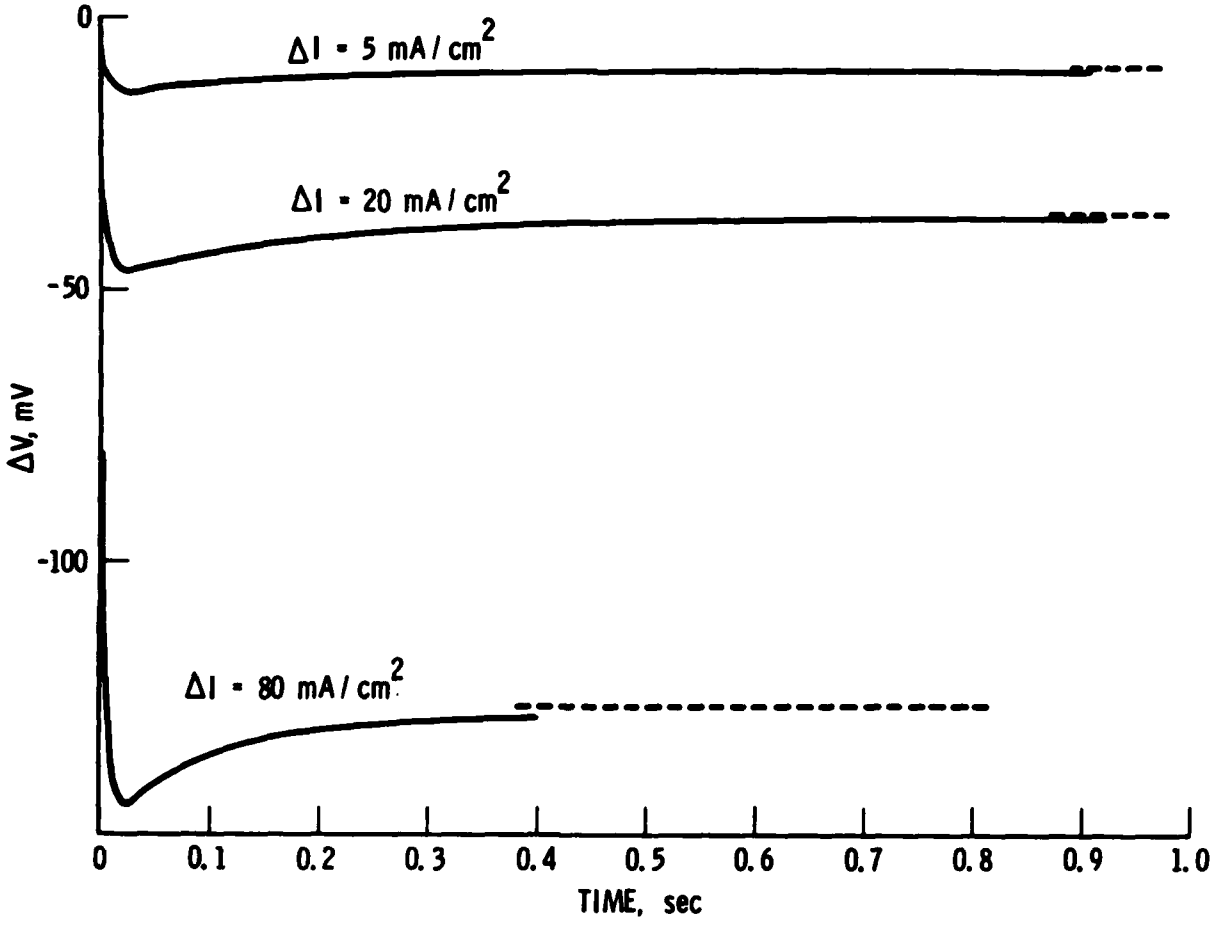

Fig. 6. Voltage Transients Calculated in Response to Different Current Steps. $b_1 = b_2 = (0.12\ V)^{-1}$, $k_2 = 1.2 \times 10^5\ cm^6\ mol^{-2}\ sec^{-1}$, $k_1/k_2 = 0.5$, $\beta = 4.4 \times 10^{-8}\ mol/cm^2$, $m = p = 2$, $[B^-] = [C^-] = 7 \times 10^{-3}\ mol/cm^3$, $\theta_i = 1.0$, $\theta_f = 0.02$, $R_s = 1.0\ \Omega$, $C_{DL} = 200\ \mu F/cm^2$. Electrode surface area was assumed 1 cm^2.

IV. CONCLUSIONS

The chemical and electrochemical reactions that can give rise to voltage-delay phenomena at active metal electrodes may be effectively modeled. Comparison of experimental data with the simple model described here should allow the adequacy of this model for various metal electrodes to be determined, and it should help suggest means of controlling passivation delay. If data are consistent with the model, the magnitude of passivation delay should be most easily affected by minimizing either the magnitude of the inductive component of the impedance or the inductive time constant τ. These minimizations may be achieved by maximizing the forward rate of reaction (1) relative to reaction (2), i.e., increasing the relative rate of the reaction that disrupts the surface coverage.

For a real electrode, several problems have not been dealt with in this simple treatment. Foremost among these is the spatial nonuniformity in current distribution on an electrode surface that is likely to develop as the surface coverage is consumed, an effect that may cause the surface area to change with time. It is possible that surface roughness, particularly as a contributor to a nonuniform current distribution, plays a major role. The importance of this and other considerations is probably best determined by empirical correlation of such models as that developed here with experimental data.

LABORATORY OPERATIONS

The Laboratory Operations of The Aerospace Corporation is conducting experimental and theoretical investigations necessary for the evaluation and application of scientific advances to new military space systems. Versatility and flexibility have been developed to a high degree by the laboratory personnel in dealing with the many problems encountered in the nation's rapidly developing space systems. Expertise in the latest scientific developments is vital to the accomplishment of tasks related to these problems. The laboratories that contribute to this research are:

Aerophysics Laboratory: Launch vehicle and reentry aerodynamics and heat transfer, propulsion chemistry and fluid mechanics, structural mechanics, flight dynamics; high-temperature thermomechanics, gas kinetics and radiation; research in environmental chemistry and contamination; cw and pulsed chemical laser development including chemical kinetics, spectroscopy, optical resonators and beam pointing, atmospheric propagation, laser effects and countermeasures.

Chemistry and Physics Laboratory: Atmospheric chemical reactions, atmospheric optics, light scattering, state-specific chemical reactions and radiation transport in rocket plumes, applied laser spectroscopy, laser chemistry, battery electrochemistry, space vacuum and radiation effects on materials, lubrication and surface phenomena, thermionic emission, photosensitive materials and detectors, atomic frequency standards, and bioenvironmental research and monitoring.

Electronics Research Laboratory: Microelectronics, GaAs low-noise and power devices, semiconductor lasers, electromagnetic and optical propagation phenomena, quantum electronics, laser communications, lidar, and electro-optics; communication sciences, applied electronics, semiconductor crystal and device physics, radiometric imaging; millimeter-wave and microwave technology.

Information Sciences Research Office: Program verification, program translation, performance-sensitive system design, distributed architectures for spaceborne computers, fault-tolerant computer systems, artificial intelligence, and microelectronics applications.

Materials Sciences Laboratory: Development of new materials: metal matrix composites, polymers, and new forms of carbon; component failure analysis and reliability; fracture mechanics and stress corrosion; evaluation of materials in space environment; materials performance in space transportation systems; analysis of systems vulnerability and survivability in enemy-induced environments.

Space Sciences Laboratory: Atmospheric and ionospheric physics, radiation from the atmosphere, density and composition of the upper atmosphere, aurorae and airglow; magnetospheric physics, cosmic rays, generation and propagation of plasma waves in the magnetosphere; solar physics, infrared astronomy; the effects of nuclear explosions, magnetic storms, and solar activity on the earth's atmosphere, ionosphere, and magnetosphere; the effects of optical, electromagnetic, and particulate radiations in space on space systems.